Surfactant Interactions with Biomembranes and Proteins

M. N. Jones
Department of Biochemistry and Molecular Biology, University of Manchester, Manchester M13 9PT

1 Introduction

Detergents are generally associated with cleaning processes from the mundane applications of dish and car washing to industrial laundering and the dispersion of oil slicks in the environment. Surface active agents (surfactants) are the main active constituents of detergent formulations. The large scale production of detergents has led to the release of surfactants into sewage treatment plants and ultimately given rise to their appearance in natural waters. Such pollution not only results in the build-up of unwanted foam at the aqueous–air interface but some surfactants present a potential toxic hazard to fish and other aquatic organisms. The realization that synthetic surfactants can be toxic, led to the development of straight-chain biodegradable surfactants and a general awareness of the need to control the contamination of natural waters by these molecules. Nowadays, the levels of surfactant contamination found in the environment are generally low and in the range 20—60 μg per litre[1] although higher levels can occur in areas where raw sewage is released.

Apart from the large scale use of detergents containing surfactants for cleaning purposes both natural surfactants such as the products of cholesterol metabolism [*e.g.* the bile acids and steroid glycosides (saponins) like digitonin and ouabain] and synthetic surfactants [*e.g.* sodium n-dodecyl sulfate (SDS) and n-octyl β-D-glucopyranoside (OBG)] have found widespread applications in biochemical research. In the biological sciences there are several major areas of research which make use of the interactions between surfactants and biological systems. These include the use of surfactants to solubilize hydrophobic components of various tissues and cellular structures, particularly membrane components. The isolation of the anion and glucose transporters of the human erythrocyte and the reconstitution of receptors for insulin, acetylcholine,[2] and the β-adrenergic receptor are all carried out by processes requiring surfactants to breakdown the interactions between the protein and the membrane lipids. The resulting soluble protein–surfactant complexes can then be handled to separate and purify the transporter or receptor before reconstituting it into a model environment such as a vesicle or liposome where function can be studied in isolation.[3,4]

One other important application of the use of a surfactant (SDS) is routine in most biochemical laboratories; this is polyacrylamide gel electrophoresis (PAGE) in SDS, *i.e.* SDS-PAGE. The technique is used to determine the polypeptide composition of proteins and depends on the formation of SDS–polypeptide complexes, which, when subjected to an electrophoretic field in a polyacrylamide gel, separate according to their molecular weights. The resulting gel is stained for protein, usually with Coomassie blue dye. This reveals the number of bands and their position on the gel, thus giving the polypeptide composition of the sample, and the molecular weights of each band with reference to a calibration, using standard proteins of known molecular weight. The procedure is carried out with reduced SDS–saturated protein complexes, *i.e.* having all their disulfide bonds reduced to −SH groups, so that ideally the surfactant binds uniformly along the polypeptide chains and the charge per unit length is constant. Since the electrical force and the frictional force on the complexes both increase with polypeptide chain length, in the absence of the cross-linked gel matrix the complexes would migrate at the same speed, but the cross-linked nature of the gel 'sieves' them and the higher molecular weight complexes are retarded. The vast majority of molecular weights for protein subunits quoted in the biochemical literature have been obtained by this technique, although it is not without its pitfalls, particularly for proteins which are partially glycosylated.[5]

All surfactants consist of a hydrophobic residue(s) terminating in a hydrophilic head group and can broadly be divided into anionic, cationic, or non-ionic depending on whether the head group is negatively, positively, or uncharged respectively. The essential feature of aqueous solutions of such amphipathic molecules is the formation of micelles above a critical concentration (the critical micelle concentration or cmc). Micelle formation is, in general, a cooperative process and the cmc represents the limiting concentration of single (monomeric) molecules that can exist in solution. The magnitude of the cmc depends on the hydrophobic–hydrophilic balance of the monomer as well as on temperature and, for ionic surfactants, on the ionic strength of the solution. Increasing ionic strength usually depresses the cmc while for many surfactants the cmc often goes through a minimum as the temperature is raised from 0 °C.[6] It was first shown by Anson in 1939[7] that many surfactants were potent denaturants of haemoglobin, but it was not until 1968 that it was established that surfactants such as SDS could form saturated complexes having approximately 1.4g of SDS per g protein (*i.e.* approximately one SDS molecule per two amino acid residues)[8] and that such binding involved interaction of the 'monomeric' surfactant with the protein.[9] This stimulated work on the precise nature of the interaction between proteins and amphipathic molecules[10—12] which is the substance of this review.

2 Interaction of Surfactants with Biomembranes

The plasma membrane is the barrier between the cytoplasm of the cell and its environment and controls the entry of metabolites and other materials into and out of the cell. In mammalian cells this is the only barrier while bacteria and plant cells also have a cell wall to maintain structural integrity, although transport is still primarily controlled by the plasma membrane. The matrix of the plasma membrane of mammalian cells is a lipid bilayer in which are embedded receptors and transporter proteins required for cell function. These are the so-called 'intrinsic proteins' in contrast to 'extrinsic proteins' which are associated with the surfaces of the bilayers. Extrinsic proteins on the cytoplasmic side of the membrane bilayer form a rigid network or cytoskeleton which helps to maintain the integrity of the membrane and in some cases its shape, while the external

Dr. M. N. Jones is a Reader in Physical Biochemistry in the Department of Biochemistry and Molecular Biology at the University of Manchester. He was trained as a chemist and his early research work was concerned with the physical properties of polymer solutions. During the late 1960s he broadened his interests to the properties of association colloids and the forces acting in thin liquid films. These studies led to work on biological membranes and model membrane systems including liposomal dispersions. His current research is concerned with biochemical thermodynamics, the properties of liposomal dispersions and their use in drug delivery, and the characterization of biological macromolecules.

surface of the plasma membrane is coated with protruding oligosaccharide chains of intrinsic membrane glycoproteins forming a glycocalyx. Figure 1 shows the structure of the human erythrocyte membrane which is probably the most studied and most comprehensively understood of all cell membranes.[12]

The lipids forming membrane bilayers in cells are complex and varied. The major constituents of the bilayer are phospholipids, sphingolipids, glycolipids, and cholesterol; bacterial cell membranes contain no cholesterol. The lipids generally have two acyl chains although some phospholipids such as cardiolipin have four. The acyl chain lengths are generally in the range C_{12} to C_{24} and have varying degrees of unsaturation. The stability of the bilayer is critically dependent on the diacyl structure which enables the acyl chains of the lipids to pack in a lamellar form with limited head-group interaction. The bilayer is one form of smectic lyotropic mesophase. If one acyl chain is removed, *e.g.* by the action of a phospholipase (often present in venoms), head-group repulsion destabilizes the bilayer relative to the micellar structure. Like surfactants, membrane lipids have an amphipathic structure but the hydrophobic–hydrophilic balance is such that the molecules are much more hydrophobic and hence the concentration of monomeric species in equilibrium with the bilayer is vanishingly small (10^{-10}—10^{-13}M). The interactions between proteins and glycoproteins and the membrane lipids are largely hydrophobic. The transmembrane sequences of membrane receptors and transporters have a high proportion of hydrophobic amino acid residues and are frequently α-helical,[13] so that the proteins are firmly anchored to the membrane but can still undergo lateral diffusion in the plane of the bilayer. It should be noted that the polypeptide chains of membrane transporters and receptors may cross the bilayer many times; the polypeptide chains of the anion transporter of the erythrocyte crosses the bilayer 14 times and the sugar transporter 12 times,[14] while numerous receptors (*e.g.* β_1 and β_2 adrenergic, M1 and M2 muscarinic, and K-receptor) fit into a family having 7 transmembrane sections.[15]

It is against this background that we must consider the interaction between surfactants and biomembranes. The simplest starting point is the isolated bilayer either in the form of a lamellar mesophase or a vesicle (liposome). Figure 2 shows the sequence of events that arise on exposing a bilayer to a typical surfactant such as SDS or the commonly used non-ionic Triton X-100 (polyethylene glycol$_{9-10}$-*p*-t-octylphenol). The effective molar ratio of surfactant to bilayer lipid (R_e) in such a system is given by equation 1.[16,17]

$$R_e = \frac{[S] - [S]_{monomer}}{[PL]} \quad (1)$$

As R_e is increased the bilayer becomes saturated with surfactant (R_e^{sat}) after which it will be progressively disrupted, the phospholipid forming mixed micelles, until the system is completed solubilized (R_e^{sol}) as mixed micelles with an increasing surfactant content, which will ultimately be in equilibrium with surfactant micelles. For surfactants with a low cmc R_e will be approximately equal to the total surfactant to phospholipid molar ratio in the system when $[S] \gg [S]_{monomer}$.

The process of bilayer disruption can be followed by using unilamellar vesicles encapsulating a radiolabelled or fluorescent solute and following its release as a function of surfactant concentration. Carboxyfluorescein is a useful tool in this respect in that at high concentration its fluorescence is quenched. If carboxyfluorescein is encapsulated in vesicles at high concentration (*i.e.* in the quenched state) its release can be followed by the increase in fluorescence due to decrease in quenching. Figure 3 shows some data for Triton X-100 release of carboxyfluorescien from egg phosphatidylcholine vesicles. The relationship between the cmc of a number of surfactants and the molar ratio of surfactant to phospholipid required to release 50% of encapsulated carboxyfluorescein (R_{50}) and to produce 50% phospholipid solubilization (S_{50}) is shown by the data in Table 1.[18] Both R_{50} and S_{50} increase with the cmc of the surfactant; there also is significant release of carboxyfluorescein below the cmc of the surfactant indicating that the surfactant monomer is incorporated into the bilayer.

The situation is considerably more complex when we come to consider surfactant interaction with a cell membrane. Figure 4 shows schematically the sequence of events on exposing a membrane to increasing amounts of surfactant.[19] The membrane bilayer initially becomes saturated with surfactant, lyses and disrupts with concomitant solubilization as lipid–protein–surfactant complexes in equilibrium with mixed micelles. On further addition of surfactant the complexes lose lipid to mixed micelles, which at sufficient high surfactant concentration will be

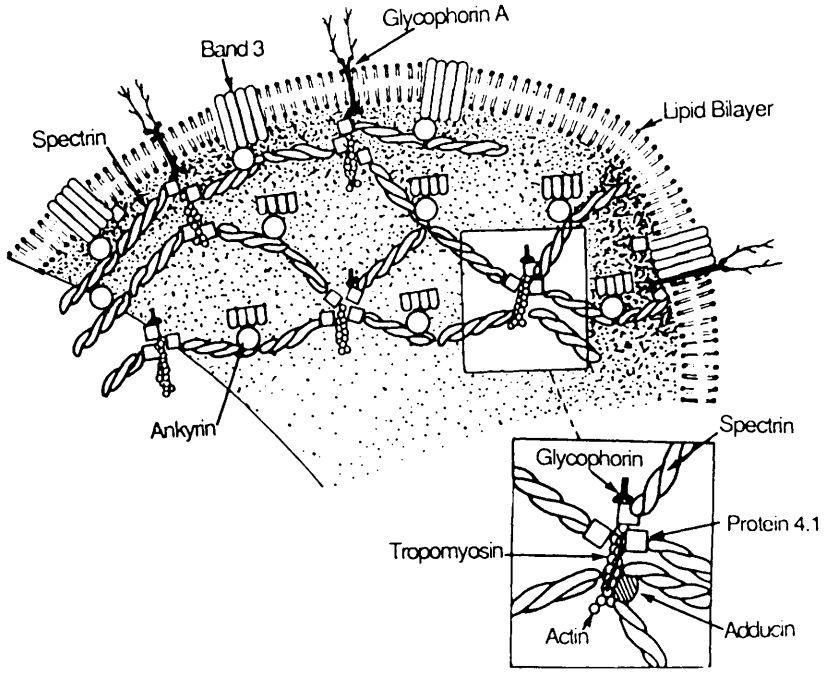

Figure 1 Schematic model of the organization of proteins and glycoproteins in the human erythrocyte membrane. (Reproduced from reference 12, p. 3, by permission of Marcel Dekker Inc.)

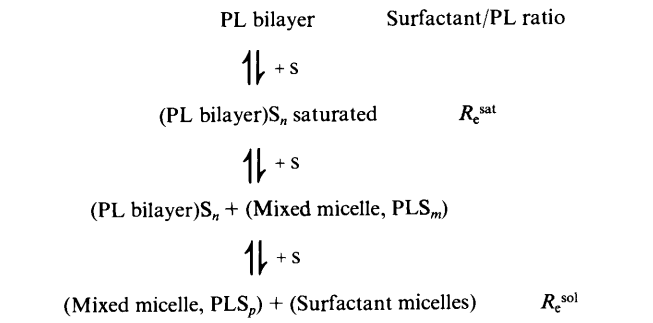

Figure 2 Schematic representation of the sequence of events arising on exposure of a phospholipid (PL) to increasing amounts of surfactant(S).

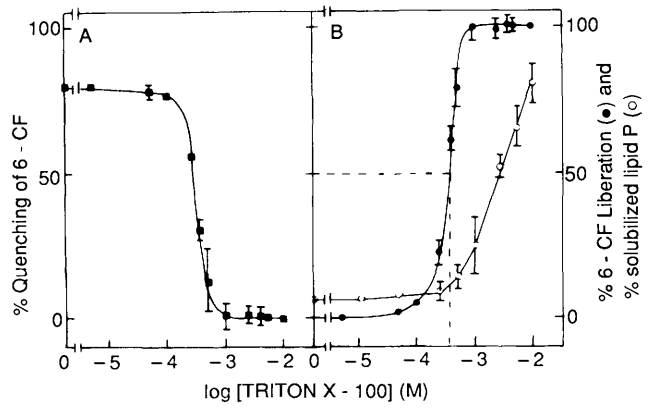

Figure 3 The release of encapsulated 6-carboxyfluorescein (6-CF) from phospholipid multilamellar liposomes by the non-ionic surfactant Triton X-100. (A) The decreases in fluorescence quenching on release of encapsulated 6-CF as a function of Triton X-100 concentration. (B) % release of 6-CF and solubilization of phospholipid as a function of Triton X-100 concentration. The dotted line shows the procedure for defining R_{50}.
(Reproduced from reference 18 by permission of Elsevier Science Publishers.)

Table 1 Surfactant release of carboxyfluorescein from phosphatidylcholine vesicles
(From Riuz *et al.*[18])

Surfactant	cmc (mM)[a]	R_{50}[b]	S_{50}[c]
Triton X-100	0.24	0.35	1.7
SDS	1.33	1.2	2.5
Sodium cholate	3.00	3.1	7.1
OBG	25.0	11.1	20.0

[a] In 0.1M NaCl. [b/c] Molar ratio of surfactant to lipid required to release 50% of encapsulated carboxyfluorescein (R_{50}) and to solubilize 50% (S_{50}) of the lipid. The final phospholipid concentration was 1mM.

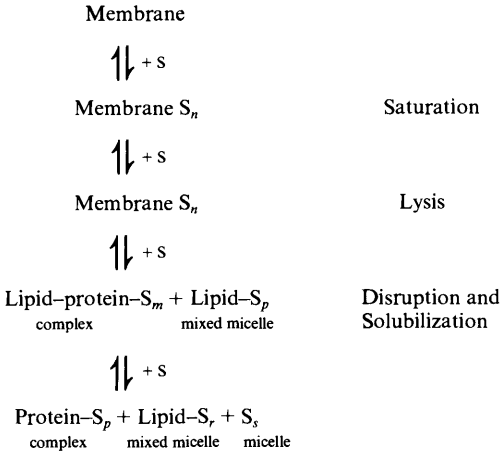

Figure 4 Schematic representation of the sequence of events arising on exposure of a biomembrane to increasing amounts of surfactant (S).

in equilibrium with surfactant micelles. The details of the membrane solubilization process will vary with the composition of the membrane but the final state, consisting of solubilized protein–surfactant complexes, demonstrates that the interactions between surfactant and proteins are in general stronger than between the proteins and membrane lipids. The detailed nature of protein–surfactant interactions can be readily studied with reference to proteins of known structure and for this it is appropriate to consider interactions between surfactants and soluble globular proteins.

3 Surfactant Interaction with Globular Proteins

The interactions between surfactants and globular proteins have been studied using a wide range of physical methods, some of which are given in Table 2 together with the type of information a technique yields. Surfactants can be broadly divided into those which bind and initiate protein unfolding, *i.e.* denaturing surfactants, and those which only bind leaving the tertiary structure of the protein intact. Commonly used anionic surfactants, such as SDS and sodium n-dodecylsulfonate, generally denature proteins whereas non-ionic surfactants do not. For this reason the non-ionics are often preferred for membrane solubilization when enzyme, receptor, or transporter function is to be preserved. There are, however, exceptions to these generalizations. Some proteins (glucose oxidase,[20] bacterial catalase,[21] papain

Table 2 Techniques used in the study of surfactant–globular protein interaction

Technique	*Information obtained*
Quantitative equilibrium dialysis	Binding isotherms, Gibbs energy of ligand binding
Molecular sieve chromatography	Binding levels
Titrimetry	Proton binding in relation to surfactant binding
Calorimetry (microcalorimetry and titration calorimetry)	Enthalpy of surfactant binding and protein unfolding
Polyacrylamide gel electrophoresis	Detection of specific complexes
Ultracentrifugation (sedimentation rate and equilibrium)	Sedimentation coefficients of protein–surfactant complexes, subunit dissociation and molecular weights
Viscometry	Hydrodynamic volume and shape factors, protein unfolding
Static and dynamic light scattering	Molecular weights, diffusion coefficients – complex dimensions
UV difference spectroscopy	Surfactant-induced conformational changes
Neutron scattering	Structure of surfactant–protein complexes
Enzyme kinetics	Surfactant-induced enzyme denaturation or activation

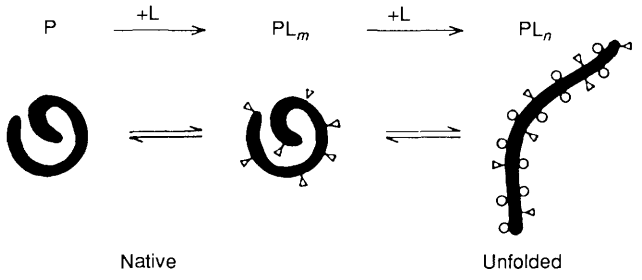

Figure 5 A schematic representation of the binding of surfactant ligands (L) to the native state of a protein P and subsequent unfolding process. (From reference 26.)

and pepsin[22] resist denaturation by SDS under some conditions and there are cases of enzyme activation by surfactants, *e.g.* *Aspergillus niger* catalase by SDS,[23] glucose-6-phosphatase by Triton X-100.[24] The bile salts sodium cholate and deoxycholate, although anionic, are non-denaturing and can activate some enzymes, *e.g.* phospholipase is activated by deoxycholate.[25]

The general pattern of interaction between surfactants and globular proteins is illustrated schematically in Figure 5. For anionic surfactants initial binding occurs to the cationic sites on the protein surface, specifically to the lysyl, histidyl, and arginyl amino acid side chains, whereas for non-ionic surfactants the binding sites will be hydrophobic patches on the protein surface and no further binding occurs after these are saturated. Anionics may, however, induce protein unfolding thus exposing many more hydrophobic binding sites previously buried in the core of the tertiary structure. The saturation of all potential binding sites is generally completed as the free surfactant concentration approaches the cmc. For reduced (no disulfide bonds) globular proteins at saturation, the protein binds between 1—2g of SDS per gram depending on the ionic strength of the solution.

Figure 6 shows typical isotherms for SDS binding to lysozyme at low and high ionic strengths. The isotherms show the average number of surfactant molecules bound to the protein ($\bar{\nu}$) as a function of the logarithm of the free surfactant concentration in equilibrium with the protein–surfactant complexes. At low free SDS concentrations the binding isotherms rise sharply as the cationic binding sites are saturated, after which binding increases more slowly before rising again as the free SDS concentration approaches the cmc. For low values of $\bar{\nu}(< 18)$ the complexes precipitate but on further binding the solutions become only turbid and for $\bar{\nu} > 30$ are optically clear.

The formation of protein–surfactant complexes (PS_n) can be represented as a series of equilibria:

$$\begin{aligned} P + S &\rightleftharpoons PS \\ PS + S &\rightleftharpoons PS_2 \\ PS_2 + S &\rightleftharpoons PS_3 \\ &\vdots \\ PS_{i-1} + S &\rightleftharpoons PS_i \\ &\vdots \\ PS_{n-1} + S &\rightleftharpoons PS_n \end{aligned} \qquad (2)$$

The equilibrium constant for the i'th step is

$$K_i = \frac{[PS_i]}{[PS_{i-1}][S]} = \frac{[PS_i]}{K_1 K_2 \ldots K_{i-1}[P][S]^i} \qquad (3)$$

The average number ($\bar{\nu}$) of surfactant molecules bound to a protein molecule is

$$\bar{\nu} = \frac{\sum_{i=1}^{n} i[PS_i]}{[P] + \sum_{i=1}^{n}[PS_i]} \qquad (4)$$

and assuming that the intrinsic binding constants for each step in equation 2 are identical apart from a statistical factor gives equation 5

$$\bar{\nu} = \frac{nK[S]}{1 + K[S]} \qquad (5)$$

This approach will not in general be valid since the binding of one surfactant molecule affects the binding of a second surfactant and so on. There are thus varying degrees of cooperativity between binding sites so that the K's are not the same. To account for this Hill[27] proposed the following expression (equation 6)

$$\bar{\nu} = \frac{n_H K[S]^{n_H}}{1 + K[S]^{n_H}} \qquad (6)$$

where n_H is the cooperativity coefficient and K an intrinsic binding constant. If binding of ligands inhibits subsequent binding, $n_H < 1$ and binding is negatively cooperative, if subsequent binding is enhanced due to the ligands already bound $n_H > 1$ and binding is positively cooperative. Figure 7 shows the way in which the shape of binding isotherms change with cooperativity for a hypothetical molecule with 50 binding sites

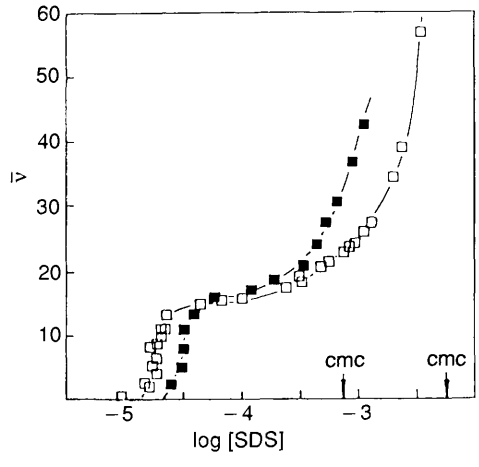

Figure 6 Binding isotherms, determined by equilibrium dialysis, ($\bar{\nu}$ *vs.* log [SDS]) for the binding of sodium n-dodecylsulphate to lysozyme in solution at 25 °C, pH 3.2; □, ionic strength 0.0119 M; ■, ionic strength 0.2119 M.

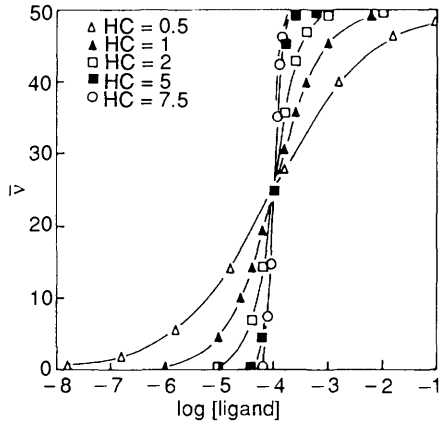

Figure 7 Theoretical binding isotherms ($\bar{\nu}$ *vs.* log [ligand]) calculated from the Hill equation for a protein with 50 binding sites (intrinsic binding constant 10^4) for a range of Hill coefficients (H.C.) from 0.5 to 7.5.
(From reference 26.)

and an intrinsic binding constant of 10^4. The isotherms become progressively steeper as n_H increases and the binding process becomes more positively cooperative.

An equation which is extensively used by biochemists is the Scatchard equation[28] which follows from equation 6, when $n_H = 1$,

$$\frac{\bar{v}}{[S]} = K(n - \bar{v}) \qquad (7)$$

The Scatchard equation would apply if all the binding sites were identical and independent. Despite its shortcomings[29] it is diagnostic of the type of cooperativity a system is displaying.[30] Figure 8 shows the Scatchard plots for the binding isotherms given in Figure 7. For $n_H < 1$ the Scatchard plots show negative curvature and for $n_H > 1$ exhibit maxima. From equation 7 it follows that $\bar{v}/[S]$ *vs.* $\bar{v}$ extrapolates to give the total number of binding sites (n) when $\bar{v}/[S] \rightarrow 0$. When the Scatchard analysis is applied to protein–surfactant interactions examples of both negative and positive cooperativity are found for some systems.

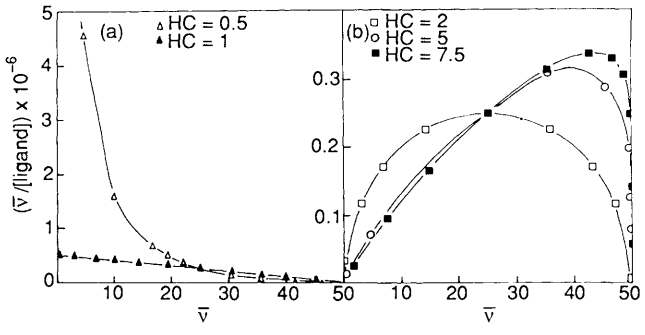

Figure 8 Theoretical Scatchard plots ($\bar{v}$/[ligand] free *vs.* $\bar{v}$) for the isotherms of Figure 7 for a protein with 50 binding sites (intrinsic binding constant 10^4) for a range of Hill coefficients from 0.5 to 7.5. (From reference 26.)

Figures 9 and 10 show Scatchard plots for the binding of SDS to bovine catalase (R.M.M. = 245 000) in acid solutions. At pH 3.2 and 4.3 curves diagnostic of negative cooperativity are obtained which extrapolate to give values of n of 343 ± 6 and 333 ± 13 respectively, which are close to the number of cationic amino acid residues in the catalase molecule of 331 (112 lysyl, 86 histidyl, and 133 arginyl). At pH 6.4 a typical positively cooperative Scatchard plot is found corresponding to a Hill coefficient of 2.61 ± 0.07. Table 3 presents data obtained by Scatchard analysis for other proteins where, like catalase, extrapolation gives values of the total number of specific binding sites very close to the number of cationic amino acid residues in the protein. The shape of the linear part of the Scatchard plots give values for the intrinsic binding constant and hence Gibbs energies of SDS binding ($\Delta G_{\bar{v}}$). Also shown in Table 3 are the corresponding enthalpies of binding per mole of SDS ($\Delta H_{\bar{v}}$) measured by microcalorimetry which combined with $\Delta G_{\bar{v}}$ give $T\Delta S_{\bar{v}}$. It can be seen that the enthalpies of binding are in general exothermic but small relative to $T\Delta S_{\bar{v}}$. The large increases of entropy on binding are characteristic of a substantial hydrophobic contribution to

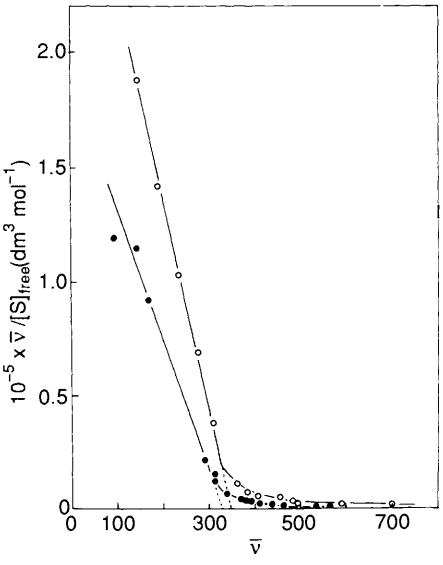

Figure 9 Scatchard plots for sodium n-dodecylsulfate (SDS) on binding to bovine catalase at 25 °C: ○, pH 3.2; ●, pH 4.3.
(Reproduced from reference 24 by permission of the publishers, Butterworth-Heinemann Ltd.)

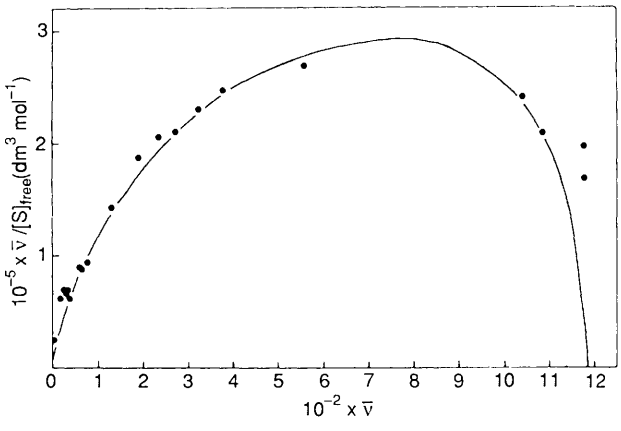

Figure 10 Scatchard plot for sodium n-dodecylsulfate (SDS) on binding to bovine catalase pH 6.4, 25 °C. The solid line was fitted using the Hill equation for a total of 1190 binding sites (1.4g SDS per g catalase) giving an intrinsic binding constant 479 ± 6 $dm^{-3}\ mol^{-1}$ and $n_H = 2.62 \pm 0.07$.
(Reproduced from reference 35 by permission of the publishers, Butterworth-Heinemann Ltd.)

the binding process arising from the disordering of water molecules, concomitant with the partial removal of the alkyl chains of the surfactant from the aqueous environment. Thus initial binding of surfactants to proteins requires not only the ionic interaction of head groups with cationic sites but also binding of the alkyl chains to hydrophobic regions of the protein in the vicinity of the cationic sites. Confirmation of this comes from the observations that chemical modification of the cationic sites, such as acetylation of lysyl residues, shifts the Scatchard

Table 3 Scatchard analysis of the binding of sodium n-dodecylsulfate to some globular proteins[31]

Protein (R.M.M.), pH	No. of cationic residues	n	K ($dm^3 mol^{-1}$)	$\Delta G_{\bar{v}}$ ($kJ mol^{-1}$)	$\Delta H_{\bar{v}}$ ($kJ mol^{-1}$)	$T\Delta S_{\bar{v}}$ ($kJ mol^{-1}$)
Ribonuclease A (13 682), 7	18	19	7.70×10^4	− 27.9	− 1.27	26.6
Lysozyme (14 306), 3.2	18	18	3.93×10^4	− 26.2	− 8.66	17.5
Ovalbumin (44 000), 7.0	42	37	1.77×10^5	− 30.0	0	30.0
Glucose oxidase (147 000), 3.7	120	132	0.51×10^4	− 21.2	− 3.29	17.9
Bovine catalase (245 000), 3.2	331	343	9.53×10^4	− 28.4	− 8.36	20.0

plots to give lower values of n, and reducing the alkyl chain length weakens binding.[32] Despite these observations any Scatchard analysis should be treated with a degree of caution, and it is not entirely clear why such a good correspondence between n and the number of cationic sites is obtained since the binding sites must only approximate to independence and are certainly not chemically identical. The pitfalls of this procedure can be seen from Figure 8a. The approximately linear portion of the curve for $n_H = 0.5$ could be extrapolated to about 12 but such an extrapolation is meaningless for this model system.

A more rigorous analysis of binding isotherms involves the use of the binding potential concept proposed by Wyman[33] in which the binding potential $\pi(P, T, \mu_1, \mu_2, \ldots)$ at pressure P and temperature T is related to the binding (ν) and chemical potential of the ligand (μ) as follows,

$$\nu = \left(\frac{\partial \pi}{\partial \mu}\right)_{P,T} \tag{8}$$

The binding potential can be calculated by integration under the binding isotherm on the assumption that the chemical potential of the ligand is given by the ideal solution expression, thus

$$\pi = RT\int_0^{\bar{\nu}} \bar{\nu}\, d\ln[S] \tag{9}$$

where R is the gas constant. Considering the formation of a specific complex (PS_n), differentiation of equations 5 with respect to ln[S] followed by substitution into equation 9 and integration gives

$$\pi = RT\ln(1 + K[S]^n) \tag{10}$$

If it is assumed that for any given free surfactant concentration a complex $PS_{\bar{\nu}}$ predominates then,

$$\pi = RT\ln(1 + K_{app}[S]^{\bar{\nu}}) \tag{11}$$

from which it is possible to calculate an apparent binding constant (K_{app}) at a given $\bar{\nu}$ and hence $\Delta G_{\bar{\nu}}$ from

$$\Delta G_{\bar{\nu}} = \frac{RT}{\bar{\nu}}\ln K_{app} \tag{12}$$

This procedure gives a profile of how $\Delta G_{\bar{\nu}}$ changes with $\bar{\nu}$. Figure 11 shows typical profiles for lysozyme and ribonuclease on interaction with SDS at pH 3.2 which demonstrates the initial 'high energy' binding at low $\bar{\nu}$ followed by progressively 'lower energy' binding as the proteins become saturated with surfactant.

Superficially these two proteins which are of very similar molecular mass and have the same number of cationic residues (18) and disulfide bonds (4) appear to bind SDS in a similar fashion with comparable Gibbs energies ($\Delta G_{\bar{\nu}}$). However, the enthalpies of interaction are significantly different as shown in Figure 12. In particular lysozyme interacts exothermically throughout the range of $\bar{\nu}$ whereas for ribonuclease interaction at low $\bar{\nu}$ is endothermic and only becomes exothermic at high binding levels. They differ markedly in the ease of unfolding, the initial endothermic interaction seen for ribonuclease arises because the endothermic enthalpy associated with surfactant-induced unfolding exceeds the exothermic enthalpy of surfactant binding, the overall enthalpy only becoming exothermic at higher binding levels. The microcalorimetry thermograms for the SDS interaction with ribonuclease clearly show both exothermic and endothermic components.[34] In contrast lysozyme has a tertiary structure which is more resistant to unfolding by SDS and only at high binding levels is there evidence of a possible endothermic contribution to the overall exothermic enthalpy of binding.

One of the most important lessons that can be learned from studies of protein–surfactant interactions is that although the overall nature of the interactions, specific-ionic interaction followed by non-specific hydrophobic interaction, is broadly similar for protein–anionic surfactant interactions the details of the process reflect the detailed tertiary structures of the proteins. It is important to note that surfactant denaturation of proteins occurs at surfactant concentrations which are far lower than those required for other commonly used denaturants such as urea (6—8 M) or guanidinium chloride (4—6 M) where the denaturation process depends primarily on the effect of the denaturant on the water structure and weakening of the hydrophobic interactions in the tertiary structure of the proteins. In thermodynamic terms the Gibbs energies of surfactant binding ($\Delta G_{\bar{\nu}}$) as saturation is approached are comparable to the Gibbs energies of micelle formation.[35] The protein–surfactant complexes saturate as the free surfactant in equilibrium with them approaches the cmc. Thus the complexes are more stable than micelles, the protein presenting a complementary amphipathic surface on which the surfactant can condense.

4 Models of Protein–Surfactant Complexes

One of the difficult aspects of the study of protein–surfactant complexes is the determination of their structure. Yonath *et al.*[36] studied the structure of lysozyme–SDS complexes by X-ray crystallography on cross-linked triclinic lysozyme crystals that had been soaked in 1.1 M SDS and then transferred to water or a lower concentration of SDS solution (0.35 M) to allow the protein to refold. It was necessary to use cross-linked crystals to prevent them dissolving on exposure to the high SDS concent-

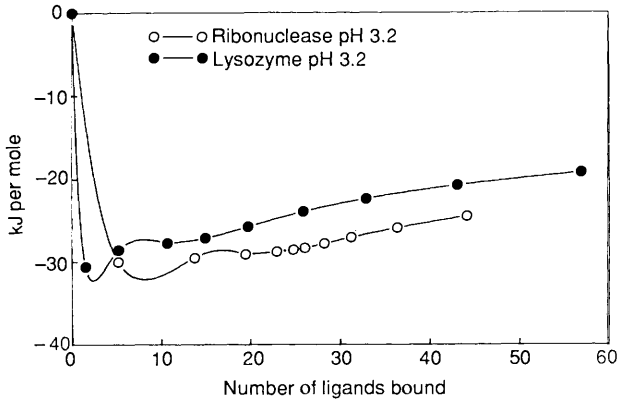

Figure 11 Gibbs energy per ligand bound ($\Delta G_{\bar{\nu}}$) as a function of number of ligands bound ($\bar{\nu}$) for lysozyme (○) and ribonuclease (●) at pH 3.2, ionic strength 0.0119 M, 25 °C.

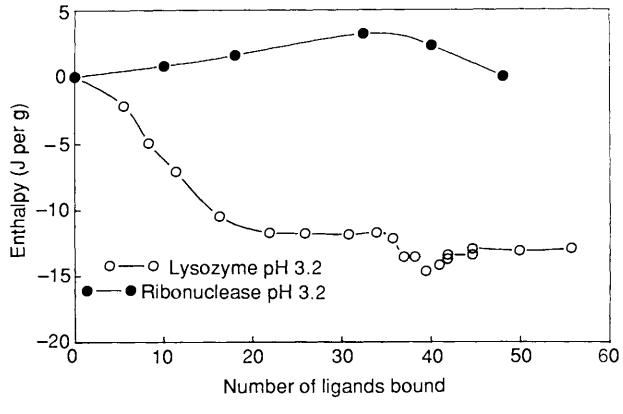

Figure 12 Enthalpy of interaction of sodium n-dodecylsufate (SDS) with lysozyme (○) and ribonuclease (●) as a function of the number of ligands bound at pH 3.2, ionic strength 0.0119 M, 25 °C.

ration. Examination of the resulting 'denatured–renatured' crystals located three SDS molecules in the renatured structure. The agreement between the structure factors of the renatured lysozyme–SDS crystals and native cross-linked crystals was 17% (renatured in water) and 19% (renatured in 0.35 M SDS) and the minimum spacings in the *X*-ray pattern of renatured and native crystals were 2.9 Å and 1.1 Å respectively. Hence the conformation of the lysozyme in the renatured crystals was similar but not identical to that of native lysozyme. The need to cross-link the crystals detracts somewhat from the significance of the results although there were only a few cross-links and these were highly flexible. The essential common feature of the complexes was the location of the SDS molecules with the sulfate head group forming a salt bridge with positively charged amino residues and the hydrocarbon chain making hydrophobic contact with the tertiary structure, consistent with the pattern of binding discussed above.

Of the three SDS molecules bound in the renatured crystal one formed a salt bridge with the terminal lysine with its alkyl chain penetrating deep into the hydrophobic core of the tertiary structure while the other two SDS molecules were bound to the protein surface, one being shared between two lysozyme molecules in the renatured crystal. The SDS molecule which penetrated into the hydrophobic core could not be removed even after soaking in SDS-free water for an extended period; however its presence did not inhibit the formation of the tertiary structure. Lysozyme has two domains separated by a cleft into which the natural substrate (cell wall polysaccharide) binds, and it is suggested that during renaturation the two domains fold separately trapping the SDS molecule between them. During denaturation many more SDS molecules will be associated with the protein but most are lost when the renatured crystal is formed.

The *X*-ray diffraction studies, while confirming the essential features of the binding process do not tell us about the structure of protein–surfactant complexes in solution when large numbers of surfactant molecules are bound. A variety of models have been proposed for the structure of SDS complexes with water-soluble proteins, usefully summarized by Ibel *et al.*[37] as follows: (a) a model in which the protein organizes the SDS anions, into a 'micelle complex'; (b) a model based on a 'rod-like particle' in which the protein forms the backbone of the complex with the SDS bound along the backbone, the particle having a length of 0.074 nm per amino acid residue; (c) a 'pearl necklace' model in which the flexible denatured polypeptide chain(s) of the protein has small spherical micelles clustered along it, the transmicellar regions of the polypeptide chain possibly forming α-helices; and (d) a 'flexible helix' model in which the SDS forms a flexible cylindrical micelle and the polypeptide chains are chemically wound around it. The stabilizing interaction proposed in this model is hydrogen-bonding between oxygens in the SDS head groups and nitrogens of the peptide bonds.[38]

The diversity of models reflect the conflicting ideas on the structure of the complexes and the difficulty of finding a technique which gives an unambiguous result. Some of the most recent work has used the neutron-scattering technique.[37,39] While this method is capable of giving much information, the results have to be fitted to models and hence the conclusions drawn from the technique are always model-dependent. The complexes formed between lithium n-dodecylsulfate and bovine serum albumin (BSA) were studied by small angle neutron-scattering.[39] BSA is a globular protein (R.M.M. = 67 000) with a single polypeptide chain and 17 disulfide linkages. The neutron-scattering data were interpreted in terms of a 'pearl necklace' model in which micelles of radius (R) equal to 1.8 nm (aggregation number 70 ± 20) were distributed along the polypeptide chain. The interparticle structure factor $S(Q)$ which takes into account interparticle correlations is given by equation 13.

$$S(Q) = 1 + N_p \int_0^\infty 4\pi r^2 \frac{g(r) \sin Qr}{Qr} dr \qquad (13)$$

N_p is the number density of spheres of radius R, and $g(r)$ is the pair-correlation function which is related to $N(r)$ the number of individual scatterers within a sphere radius r.

$$g(r) = \frac{1}{4\pi r^2}\left(\frac{dN}{dr}\right) \qquad (14)$$

$N(r)$ can be related to the fractal dimension (D) of the protein–surfactant complex by the relation $N(r) = (r/R)^D$. Since the distribution of micelles is dictated by the topology of the polypeptide backbone the fractal dimension is lower than 3, as it would be for freely diffusing micelles provided there were no intermicellar correlations. Thus the fractal dimension can be taken as an index of the topology of the surfactant-denatured protein. For increasing concentrations of dodecylsulfate (wt.%) the fractal dimension decreases from 2.3 (1%), to 1.76 (3%) consistent with the a transition from a compact state to a more open random coil in which a string of constant-sized micelles are distributed along the hydrophobic patches of the denatured random coil.

The 'pearl necklace' model for the BSA–dodecylsulfate complexes is different from the model which has been reported for the structure of the complexes formed between the deuterated bifunctional enzyme *N*-5′-phosphoribosylanthranilate/indole-3-glycerol-phosphate synthase (PRA-IGP) and SDS.[37] This enzyme from *Escherichia coli* contains a single polypeptide chain of 452 amino acids (R.M.M. = 49 484) with no disulfide bonds. The deuterated molecule binds 1.26 g SDS per g protein (216 SDS molecules/452 amino acid residues). Neutron scattering was investigated from the whole molecule complex (W) and two SDS-complexed fragments produced by gentle hydrolysis with trypsin, a large fragment (L) containing 289 residues and a small fragment (S) containing 163 residues. Figure 13 shows the pair–distance distribution functions (PDDFs) of volume elements of the three SDS-complexed structures at vanishing contrast between the buffer-medium and the protein–surfactant phase. The small complex (S) gives a single peak corresponding to a single globular structure and a neutron scattering total dodecyl-chain volume (V_c) of 26.0 ± 1 nm^3 and 73 ± 3 $C_{12}H_{25}$ chains. The large complex (L) gives two peaks which arise from two micelles associated with the C- and N-terminal ends of the polypeptide chain (L_C and L_N) which are well separated. The first peak (the self peak) is due to interferences of pairs of volume elements within the same micelle and the second peak is due to

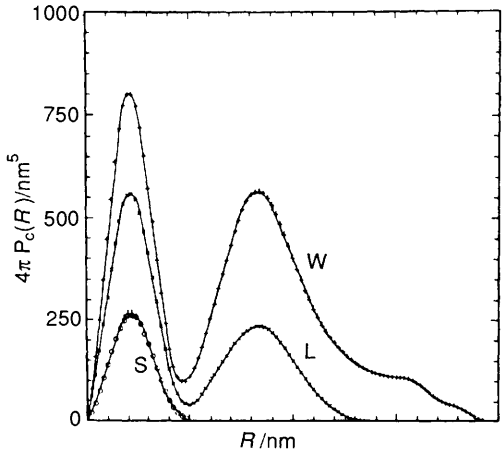

Figure 13 Pair–distance distribution functions (PDDFs) of volume elements situated in n-dodecylsulfate phases of SDS-(*N*-5′-phosphoribosylanthranilate isomerase/indole-3-glycerol-phosphate synthase) complexes as observed by neutron scattering at vanishing contrast between the buffer and the protein–SDS phase. S (small fragment, R.M.M. = 17 478; 163 amino acid residues. L (large fragment, R.M.M. = 32 024; 289 amino acid residues. W (whole molecule, R.M.M. = 49 484; 452 amino acid residues).
(Reproduced by permission from reference 37.)

interferences of pairs of volume elements in the micelles associated with L_C and L_N; for these V_c is 35.6 ± 1.5 nm^3 (101 ± 4 SDS molecules) and 14.7 ± 0.8 nm^3 (42 ± 2 SDS molecules) respectively. The whole molecule complex (W) gives two peaks and a shoulder. These are intepreted as the self peak (at low R), the central peak arising from interferences between pairs of volume elements situated in the core of a central micelle (W_M) and the core of a micelle associated with either the C-terminal (W_C) or N-terminal (W_N) ends of the polypeptide chain, and finally the shoulder (at large R) arising from intereference between pairs of volume elements in W_C and W_N. The number of SDS molecules in the three micelles W_M, W_C, and W_N are approximately 42, 101, and 73 respectively, giving the proposed structure shown in Figure 14 in which the polypeptide chain is wrapped around the three micelles to give what is described as a 'protein-decorated micelle' structure. In the structure it is assumed that the two interconnecting polypeptide segments, which may bind a small number of SDS molecules, are highly flexible as in the 'pearl necklace' model, and that the repulsive interaction between the micelles leads to an overall elongated conformation.

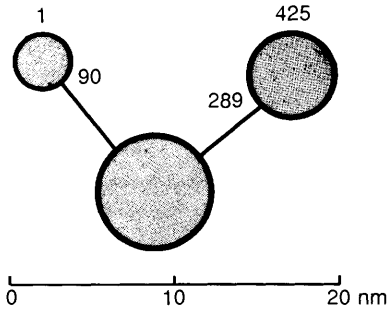

Figure 14 'Protein-decorated micelle' model of the complexed formed between 216 sodium n-dodecylsulfate molecules and the 452 amino acid residues of *N*-5'-phosphoribosylanthranilate isomerase/indole-3-glycerol-phosphate synthase. The complex consists of three spherical micelles (grey areas) mostly of SDS alkyl chains with hydrophilic shells (black areas) occupied by polypeptide chains and sulfate head groups.
(Reproduced by permission from reference 37.)

There is clearly a considerable difference between the 'pearl necklace' and 'decorated micelle' models which may in part relate to the differences between the proteins, in particular the fact that BSA has a more restricted conformation because of disulfide linkages. The most important difference is that in the 'pearl necklace' model the polypeptide chain is believed to pass through micelles of constant size as opposed to around micelles of variable size in the 'decorated micelle' model. However, it is significant that for the decorated micelles the number of SDS molecules per amino acid residue are surprisingly uniform 0.45(S), 0.49(L), and 0.48(W).

The structure of protein–non-ionic surfactant complexes is not in general complicated by protein unfolding and there seems little alternative but to envisage the binding of the surfactant molecules to hydrophobic patches on the protein surface. The binding of OBG to globular proteins has become a controversial issue in that no evidence for binding was found using molecular sieve chromatography[40] whereas equilibrium dialysis gave binding levels consistent with the formation of complexes in which the OBG adsorbed as a monolayer on the protein surface. For globular proteins covering a molecular weight range from 14 000 to 350 000,[41] as the free OBG concentration approached the cmc, the binding levels increased with protein size and for many proteins the extent of binding calculated assuming the proteins are ellipsoidal in shape and coated with surfactant molecules agreed well with the experimentally measured binding levels at the cmc of the OBG.

5 Molecular Dynamics of Protein–Surfactant Complexes

A recent development in the study of protein–surfactant complexes is the application of the technique of molecular dynamics.[42] From a knowledge of the potential functions describing the molecular interactions in a protein, the force on each atom at some time t can be calculated. By use of Newton's equations of motion it is then possible to calculate the acceleration of each atom and by iterative integration the velocity and position of each atom at time $t + \delta t$, where δt is of the order of 1 fs. By performing tens of thousands of such iterations the motion of the protein over a time period of 10—1000 ps can be followed which is sufficient to find the conformation of minimum energy. In principle such calculations should be carried out including a large number of water molecules but in practice the computational time required to include even a few tens of water molecules is often prohibitively long. The aqueous environment can be approximated to by using a radially dependent permittivity.

Figure 15 shows a computer simulation of the proteins ribonuclease and lysozyme with ten bound SDS molecules at pH 3. The potential energies of binding are shown in Figure 16 and predict that SDS should have a greater affinity for lysozyme than for ribonuclease, particularly for the first two to three SDS molecules bound. This prediction is borne out by the experimental values of $\Delta G_{\bar{v}}$ for very low values of $\bar{v}$ (Figure 11), although at higher values of $\bar{v}$ binding to ribonuclease is stronger (lower energy) than binding to lysozyme. Furthermore it is interesting that although these two proteins have structural similarities such as size and the number of disulfide linkages the structural disorganization caused by the binding of the surfactant ligands is considerably greater in the case of ribonuclease than it is for lysozyme. Figure 17 shows the native conformation of the two proteins on which has been superimposed the minimum energy conformation of the polypeptide chain after ten surfactant ligands have been bound. The change in conformation relative to the native state is clearly considerably larger for ribonuclease than for lysozyme as reflected in the root-mean-square (RMS) displacements of all the atomic positions as a function of binding (Figure 18). It is significant that the enthalpies of interaction of the two proteins with SDS (Figure 12) clearly reflect the differences in the rigidity of their structures as suggested by the molecular dynamic calculations. The endothermicity of the initial interaction for ribonuclease, associated with a conformational change, contrasts with the exothermicity of the interaction of SDS with the more rigid conformation of lysozyme. Although the problem of taking account of water molecules is not fully addressed in the molecular dynamic calculations the correspondence between the theoretical predictions and the experimental observations are sufficiently encouraging to suggest that this approach can be usefully applied to protein–surfactant interactions and should yield worthwhile results in the future.

6 References

1 M. A. Lewis and V. T. Wee, *Environmental Toxicology and Chemistry*, 1983, **2**, 105.
2 O. T. Jones, J. P. Earnest, and M. G. McNamee, in 'Biological Membranes', ed. J. B. C. Findlay and W. H. Evans, IRL Press, Oxford, 1987, Chapter 5, p. 139.
3 J. K. Nickson and M. N. Jones, *Biochim. Biophys. Acta*, 1982, **690**, 31.
4 M. N. Jones, J. E. More, and D. J. Riley, *J. Receptor Res.*, 1986, **6**, 361.
5 K. Weber and M. Osborn, *J. Biol. Chem.*, 1969, **244**, 4406.
6 R. J. Hunter, 'Foundation of Colloid Science', Volume 1, Clarendon Press, Oxford, 1987, Chapter 10, 564.
7 M. L. Anson, *Science*, 1939, **90**, 256.
8 R. Pitt-Rivers and F. S. A. Impiombato, *Biochem. J.*, 1968, **109**, 825.
9 J. A. Reynolds and C. Tanford, *Proc. Natl. Acad. Sci., USA*, 1970, **66**, 1002.
10 J. Steinhardt and J. A. Reynolds, 'Multiple Equilibrium in Proteins', Academic Press, New York, 1969.

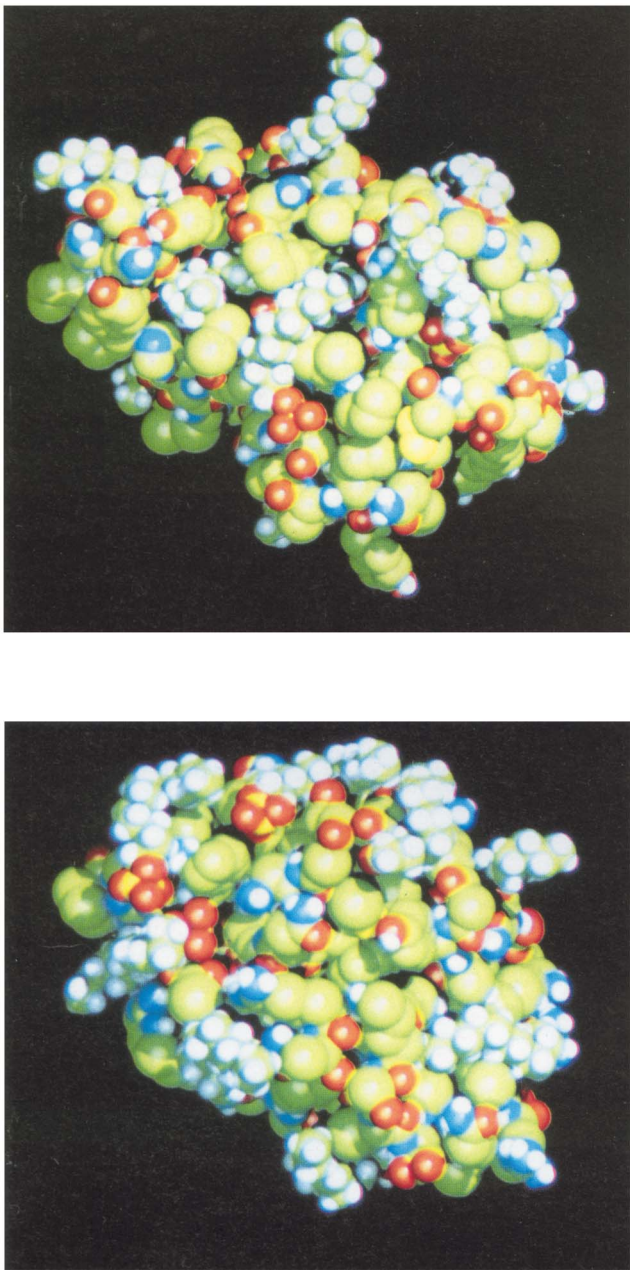

Figure 15 Molecular dynamic simulations of the structure of ribonuclease (a) and lysozyme (b) sodium n-dodecylsulfate (SDS) complexes with 10 surfactant ligands bound at pH 3. The hydrogens of the SDS alkyl chains are white; sulfur, yellow; oxygen, red; carbon, green; nitrogen blue.

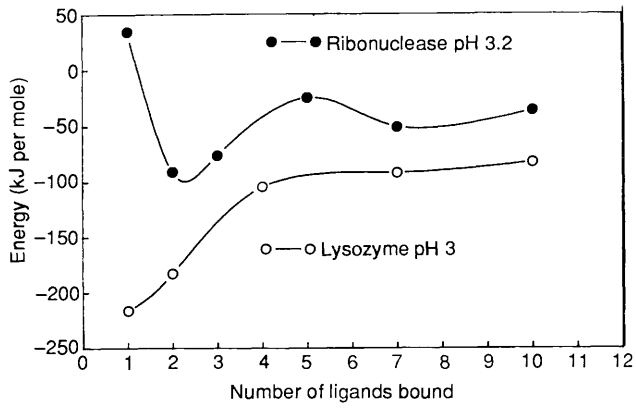

Figure 16 Minimized potential energies of interaction of sodium n-dodecylsulfate (SDS) ligands (energy per ligand bound) with ribonuclease and lysozyme at pH 3.

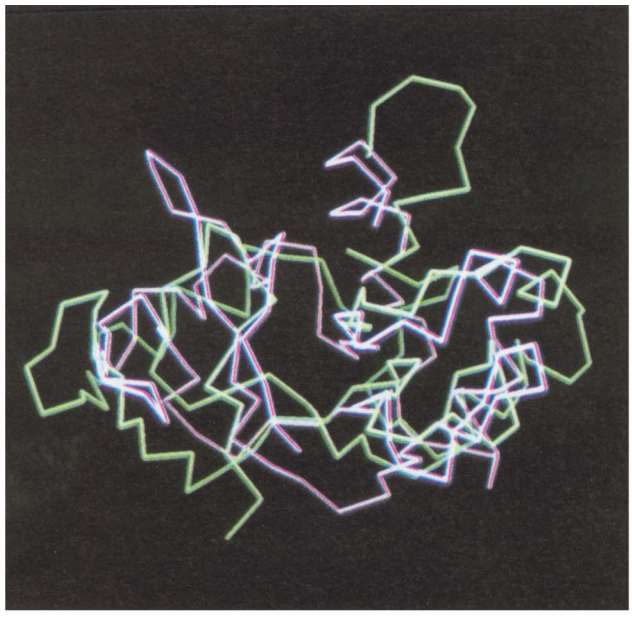

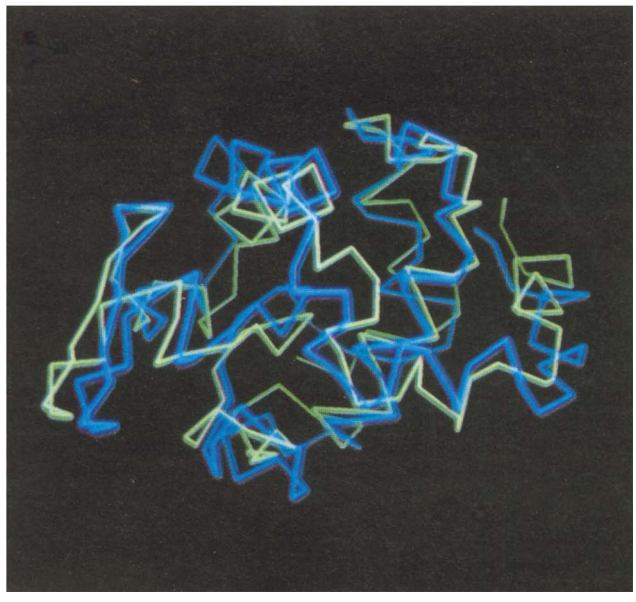

Figure 17 (a) Polypeptide chain conformation of native ribonuclease (pink) and the ribonuclease $(SDS)_{10}$ complex (green). (b) Polypeptide chain conformation of native lysozyme (blue) and lysozyme $(SDS)_{10}$ complex (green) at pH 3.

11 M. N. Jones, 'Biological Interfaces', Elsevier, Amsterdam, 1975, Chapter 5, p. 101.
12 P. Agre and J. C. Parker, 'Red Blood Cell Membranes: Structure, Function, Chemical Implications', Marcel Dekker, New York, 1989, Chapter 1.
13 D. M. Engleman, T. A. Steitz, and A. Goldman, *Ann. Rev. Biophys. Biophys. Chem.*, 1986, **15**, 321.
14 D. J. Anstee, *Vox Sang.*, 1990, **58**, 1.
15 Y. Masu, K. Nakayama, H. Tamaki, Y. Harada, M. Kuno, and S. Nakanishi, *Nature*, 1987, **329**, 836.
16 D. Lichtenberg, R. J. Robson, and E. A. Dennis, *Biochim. Biophys. Acta*, 1983, **737**, 285.
17 D. Lichtenberg, *Biochim. Biophys. Acta*, 1985, **821**, 470.
18 J. Ruiz, F. M. Goni, and A. Alonso, *Biochim. Biophys. Acta*, 1988, **937**, 127.
19 A. Helenius and K. Simons, *Biochim. Biophys. Acta*, 1975, **425**, 29.

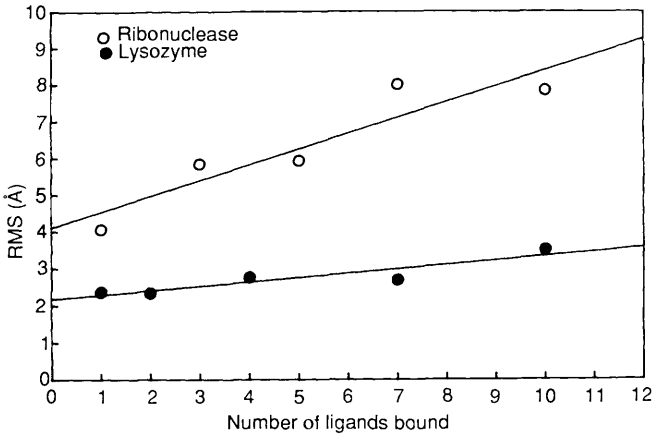

Figure 18 Root-mean-square displacements (RMS) of the polypeptide chains of ribonuclease and lysozyme sodium n-dodecylsulfate (SDS) complexes as a function of the number of SDS ligands bound at pH 3.

20 M. N. Jones, P. Manley, and A. E. Wilkinson, *Biochem. J.*, 1982, **203**, 285.
21 M. N. Jones, P. Manley, P. J. W. Midgley, and A. E. Wilkinson, *Biopolymers*, 1982, **21**, 1435.
22 C. A. Nelson, *J. Biol. Chem.*, 1971, **246**, 3895.
23 M. N. Jones, A. Finn, A. Mosavi-Movahedi, and B. J. Waller, *Biochim. Biophys. Acta*, 1987, **913**, 395.
24 F. E. Beyhl, *IRCS Med. Sci.*, 1986, **14**, 417.
25 M. Y. El-Sayert and M. F. Roberts, *Biochim. Biophys. Acta*, 1985, **831**, 133.
26 M. N. Jones and A. Brass, in 'Food Polymers, Gels, and Colloids', ed. E. Dickinson, Special Publication No. 82 The Royal Society of Chemistry, Cambridge, 1991, p. 65.
27 A. V. Hill, *J. Physiol.*, 1910, **40**, 40P.
28 G. Scatchard, *Ann. N.Y. Acad. Sci.*, 1949, **51**, 660.
29 I. M. Klotz and D. L. Hunston, *J. Biol. Chem.*, 1984, **259**, 10060.
30 G. Schwarz, *Biophys. Struct. Mech.*, 1976, **2**, 1.
31 M. N. Jones, in 'Biochemical Thermodynamics', ed. M. N. Jones, Elsevier, Amsterdam, 1988, Chapter 5, p. 228.
32 M. N. Jones and P. Manley, *J. Chem. Soc., Faraday Trans. 1*, 1980, **76**, 654.
33 J. Wyman, *J. Mol. Biol.*, 1965, **11**, 631.
34 M. I. Paz Andrade, E. Boitard, M. A. Saghal, P. Manley, M. N. Jones, and H. A. Skinner, *J. Chem. Soc., Faraday Trans. 1.*, 1981, **77**, 2939.
35 M. N. Jones and P. Manley, *Int. J. Biol. Macromol.*, 1982, **4**, 201.
36 A. Yonath, A. Podjarny, B. Honig, A. Sielecki, and W. Traub, *Biochemistry*, 1977, **16**, 1418.
37 K. Ibel, R. P. May, K. Kirschner, H. Szadkowski, E. Mascher, and P. Lundahl, *Eur. J. Biochem.*, 1990, **190**, 311.
38 P. Lundahl, E. Greijer, M. Sandberg, S. Cardell, and K. D. Eriksson, *Biochim. Biophys. Acta*, 1986, **873**, 20.
39 S.-H. Chen and J. Teixeira, *Phys. Rev. Lett.*, 1986, **57**, 2583.
40 P. Lundahl, E. Mascher, K. Kameyama, and T. Takagi, *J. Chromatogr.*, 1990, **518**, 111.
41 J. Cordoba, M. D. Reboiras, and M. N. Jones, *Int. J. Biol. Macromol.*, 1988, **10**, 270.
42 J. A. McCammon and S. C. Harvey, 'Dynamics of Proteins and Nucleic Acids', Cambridge University Press, Cambridge, 1987.